

## SIGNIFICANCE OF BEATING OBSERVED IN EARTHQUAKE RESPONSES OF BUILDINGS

Mehmet Çelebi<sup>1</sup>, S. Farid Ghahari<sup>2</sup>, and Ertuğrul Taciroğlu<sup>2</sup>  
U.S. Geological Survey<sup>1</sup> and University of California, Los Angeles<sup>2</sup>  
Menlo Park, California, USA<sup>1</sup> and Los Angeles, California, USA<sup>2</sup>

### Abstract

The beating phenomenon observed in the recorded responses of a tall building in Japan and another in the U.S. are examined in this paper. Beating is a periodic vibrational behavior caused by distinctive coupling between translational and torsional modes that typically have close frequencies. Beating is prominent in the prolonged resonant responses of lightly damped structures. Resonances caused by site effects also contribute to accentuating the beating effect. Spectral analyses and system identification techniques are used herein to quantify the periods and amplitudes of the beating effects from the strong motion recordings of the two buildings. Quantification of beating effects is a first step towards determining remedial actions to improve resilient building performance to strong earthquake induced shaking.

### Introduction

In a cursory survey of several textbooks on structural dynamics, it can be seen that beating effects have not been included in their scopes. On the other hand, as more earthquake response records from instrumented buildings became available, it also became evident that the beating phenomenon is common. As modern digital equipment routinely provide recordings of prolonged responses of structures, we were prompted to visit the subject of beating, since such response characteristics may impact the instantaneous and long-term shaking performances of buildings during large or small earthquakes. The main purpose in deploying seismic instruments in buildings (and other structures) is to record their responses during seismic events to facilitate studies understanding and assessing their behavior and performances during and future strong shaking events. Beating phenomenon falls into such a response characteristic that needs to be understood.

Beating is a periodic, resonating and prolonged vibrational behavior caused by distinctive close coupling of translational and torsional modes of a lightly damped structure (Boroschek and Mahin, 1991, Çelebi, 1994, 1997). Thus, repetitively stored potential energy during the coupled translational and torsional deformations turns into repetitive vibrational energy, causing the ensuing prolonged motions. The energy periodically flows back and forth between closely coupled modes and mostly with regular periodicity. The coupled motions reinforce and weaken each other. Figure 1 demonstrates two simple harmonic signals with constant frequencies (0.45 and 0.57 Hz) and with and without light damping ratio of 1 %, are summed to demonstrate the beating phenomenon. The “beat frequency” ( $f_b$ ) - as it is generally referred to in acoustical physics - is denoted by the absolute value of the differences in frequencies ( $f_1-f_2$ ) that cause the phenomenon [[https://en.wikipedia.org/wiki/Beat\\_\(acoustics\)](https://en.wikipedia.org/wiki/Beat_(acoustics))]. The “beating period” ( $T_b$ ) is twice the inverse of beat frequency ( $T_b=2/f_b$ ) as shown in Figure 1. Throughout this paper, the beating period will be computed by the following equation (see also Boroschek and Mahin, 1991):

$$T_b = \frac{1}{f_b} = \frac{2}{|f_1 - f_2|} = \frac{2T_1 T_2}{|T_1 - T_2|} \quad (1)$$

Of course, it is understood that the real-life response of a structure is not this simple. The amplitudes of reinforcing signals vary drastically and there may be additional signals from other modes that further complicate the resulting response and visual identification of the beating period.

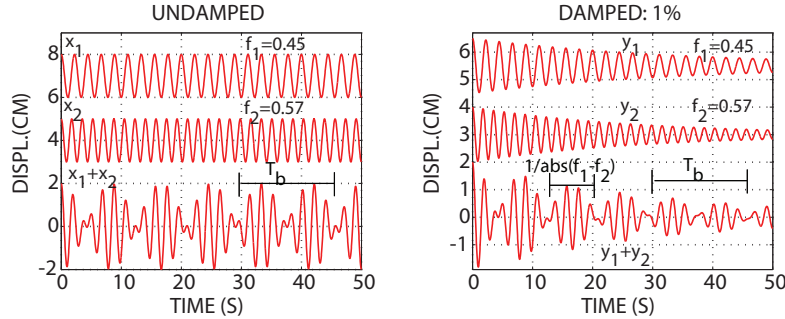


*Figure 1. Illustration of the beating effect produced by the summing of two harmonic signals (0.45 and 0.57 Hz respectively) with different amplitudes for both undamped (left) and damped (right) conditions. When added, the signals reinforce or weaken and demonstrate the definition of beating period.*

In several case studies it was noted that resonance caused by site effects also contributes to beating effect (e.g. Çelebi et al., 2014). Thus it becomes necessary to determine site frequencies to infer possible resonance that can be caused by closeness of the site frequency to the structural frequency – as demonstrated for Case 1 (below) where site transfer function is computed using shear wave velocity ( $V_s$ ) versus depth profiles of the site of that building (Çelebi et al., 2014).

Engineering implications of the beating effects are: (a) Prolonged cyclic shaking due to beating effect takes its toll on the structural system – particularly if the structure is brittle and old (historical buildings), (b) Repetitive shaking accentuates fatigue and low-cycle fatigue, and (c) Beating cycles can cease functionality of a building or cause serious discomfort to occupants (as it did in Case 1). The purpose of this paper is to review previous studies and when applicable, present new results from further analyses of two buildings whose responses consistently exhibit beating during earthquakes. Such studies can lead to development and/or use of design and construction methods to attenuate or eliminate negative impact caused by beating effect and, as a result, improve their resiliency. Throughout the paper, spectral analyses methods described by Bendat and Piersol (1980) and system identification procedures described by Ljung (1987) are used. System identification allows computation of modal damping values in addition to the modal frequencies.

### **Case 1: 55-Story Building in Osaka, Japan during Tohoku Earthquake**

Unprecedented long duration response records were retrieved from a 55-story tall building located 769 km from the epicenter of the mainshock of the M9.0 March 11, 2011 Tohoku, Japan earthquake (<http://earthquake.usgs.gov/earthquakes/eqintheneWS/2011/usc0001xgp/>, last visited July 15, 2011). Vertical sections of the building, a typical plan view and locations of tri-axial accelerometers are shown in Figure 2. In a separate study, Çelebi and others (2014) provide a detailed study of the mainshock as well as numerous aftershock records of the building including discussions of average drift ratios as related to performance. In this paper, we discuss only beating effects as observed from only the mainshock records. The fact that the shaking of the building was both strong and prolonged caused the loss of functionality of the building and significant problems for the occupants and visitors.

The building response records echo also the consistent long-duration strong shaking characteristics of the hundreds of surface and downhole (mainshock and aftershock) free-field records publicly released by the dense surface and downhole seismic instrument networks (K-Net and KiK-Net) of Japan (<http://www.kyoshin.bosai.go.jp/>, last visited April 21, 2016). In addition, site transfer functions computed from geotechnical logs of KIKNET station OSKHO2, the free-field station closest to the building (~2.5 km), confirms the possibility of resonance due to soil-structure interaction (SSI) – which was not considered during the design/analysis phase of the building. Towards this possibility, we compute

the site transfer functions using software developed by C. Mueller (*pers. comm.*, 1997), which is based on Haskell's shear wave propagation method (Haskell, 1953 and 1960). In this method, the transfer function is computed using linear propagation of vertically incident SH waves, and has, as input, data related to the layered media (number of layers, depth of each layer, corresponding Vs, damping, and density), desired depth of computation of transfer function, computation frequency (df), half space substratum shear wave velocity and density. Damping ( $\xi$ ) in the software is introduced via the quality factor (Q), a term used by geophysicists that is related to damping by  $\xi = 1/(2Q)$ . The parameters used in computing the site transfer functions are the Profiles A, B, and C shown in Figure 3. Profile A is an approximation based on the geotechnical data for free-field KiK-Net station OSKH02 that is near (~2.5km) the building. In this profile, the upper and softer layers have been ignored. By way of comparison with the transfer functions computed for Profiles B and C, which underlie the building, it is concluded that the upper layers do not significantly alter the computed fundamental frequency of the site of this building. Q values used in calculating the transfer functions range between 25-60 for shear wave velocities between 200-600 m/s – having been approximately interpolated to vary linearly within these bounds. As seen in Figure 3, the fundamental frequency of the site is computed to be in the range of 0.13-0.17 Hz due to the dominant characteristics of layers 3 and 4 (typically of the area of the site of the building and KiK-Net OSKH02 strong-motion station as described in Figure 3).

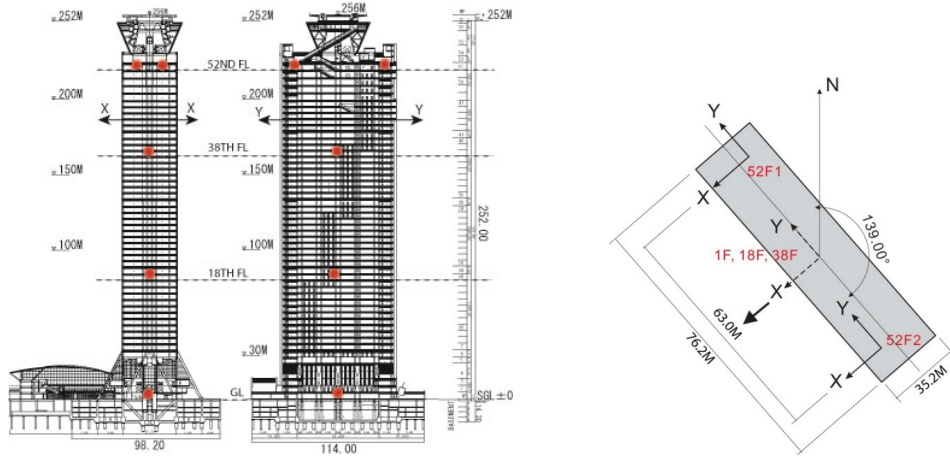


*Figure 2. (left) Vertical sections of the building showing major dimensions and locations of tri-axial accelerometers on the 52nd, 38th, 18th and ground level (1st Floor). (right) Principal axes of the building in plan view showing locations and orientations of the sensors on 52nd, 38th, 18th and ground levels.*

Next, we use building response records to compute structural frequencies. Figure 4 displays the unprecedented 1000 s-long recorded acceleration time-histories (in both X [219] and Y [319] directions) at 1<sup>st</sup> floor (as input) and at 52<sup>nd</sup> floor (as output) as well as the computed 52<sup>nd</sup> floor accelerations using system identification. To the best knowledge of the authors, such long-duration response records have not previously been obtained, even though there likely have been many buildings that experienced such shaking. The long durations of repetitious cycles in the responses suggest that the building is in resonance. This is also supported by the fact that the site frequency (between 0.13-0.17Hz) is very close to the fundamental frequencies of the building (~0.15Hz) as exhibited in amplitude spectra in Figure 4. The amplitude spectra and spectral ratios (Figure 5) further confirm these structural frequencies.

In addition, the damping percentages extracted from system identification analyses (Table 1) are quite low (1.2 and 1.6 % in X and Y directions, respectively) which is herewith asserted to be one of the main causes for the prolonged shaking, including beating phenomenon particularly in the Y-direction of the building. The computed low damping values are also supported by the very narrow bandwidths of the

dominant peaks in the amplitude spectra of both the recorded and computed accelerations (Figures 4, 5).

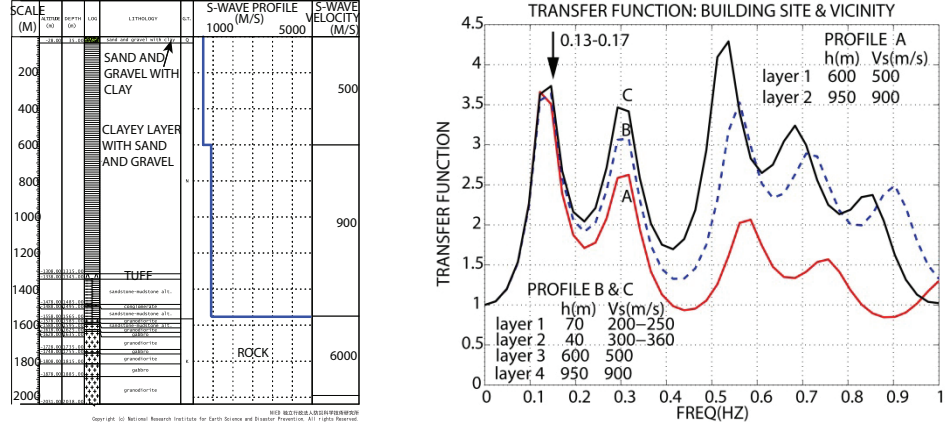


Figure 3. (Left) Depth versus  $V_s$  profile of the OSKH02 KiK-Net site (modified from NIED, 2011: [www.kik.bosai.go.jp/](http://www.kik.bosai.go.jp/), last visited 09/16/2011). (Right) Transfer functions computed for Profile A (near the OSKH02 strong-motion site) and Profiles B and C below the building. The depth of the softer upper two layers (to about 1500 m depth) below the building does not affect the fundamental mode of the site.

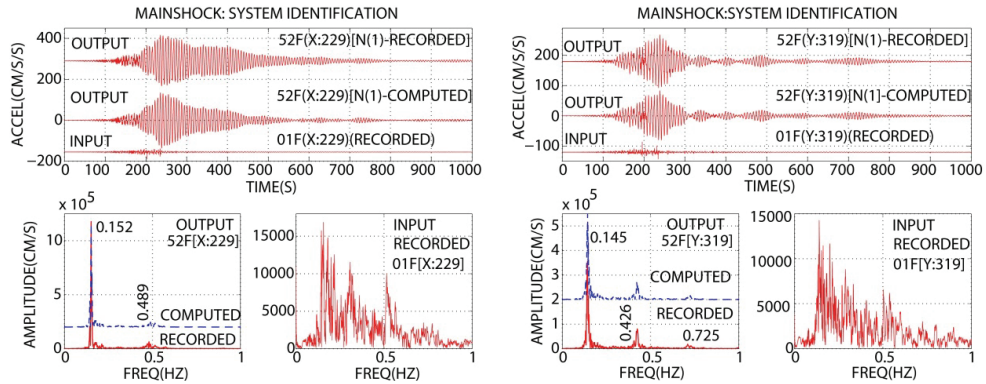


Figure 4. System identification applied to mainshock records in the X (229) and Y (319) directions. The first floor accelerations are used as input and the 52nd floor accelerations as output. The computed 52nd floor accelerations match well with the recorded. System identification also facilitates computation of the modal damping ratios. Amplitude spectra peaks at the 52<sup>nd</sup> floor are very narrow – indicative of low damping.

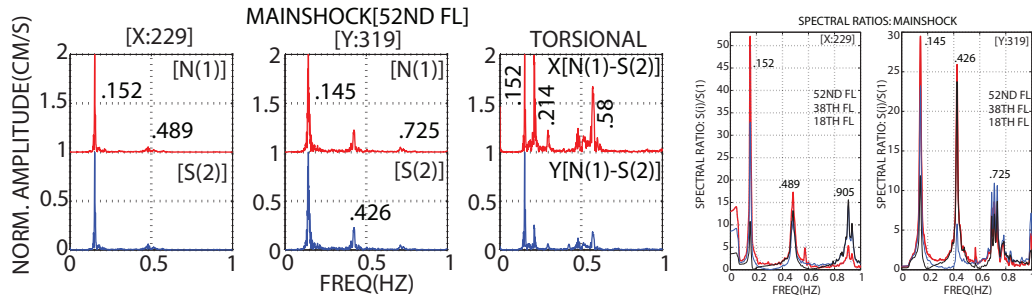


Figure 5. (left) Amplitude spectra of accelerations at the 52nd floor exhibit the frequencies in principal axes of the building. Torsional frequencies are identified from the difference (N-S) between two parallel accelerations at the 52F1 and 52F2 locations (Figure 2). Third mode (~0.9 Hz) in X-direction is not

*identified from amplitude spectrum, but is identified by spectral ratios (right) of the amplitude spectra of the 52<sup>nd</sup>, 38<sup>th</sup> and 18<sup>th</sup> floors with respect to the 1<sup>st</sup> level.*

**Table 1. Summary of Frequencies [Periods] Determined by Spectral Analyses and System Identification Applied to Mainshock. Critical Damping Percentages are Identified by System Identification Only.**

Orientation	X [229]			Y [319]			Torsion	
	Modes	1	2	3	1	2	3	1
<i>MAINSHOCK /EVENT 1/ (Spectral Analysis)</i>								
Freq. (Hz) [T (s)]	0.152 [6.58]	0.489 [2.06]	0.905 [1.11]	0.145 [6.90]	0.426 [2.34]	0.725 [1.38]	.213 [4.69]	.58 [1.72]
<i>MAINSHOCK /EVENT 1/ (System Identification)</i>								
Freq. (Hz) [T (s)]	0.1524 [6.56]	0.4887 [2.05]	N/A	0.1447 [6.91]	0.4264 [2.35]	0.7250 [1.38]		
Damping ratio ( $\xi$ )	0.012	0.020		0.016	0.001	0.020		

Denoting the identified translational fundamental periods (Table 1) of the building as T1 (6.58 s or 6.9 s) in the X- or Y-directions respectively, and torsional period as T2 (4.69 s), then, using equation 1 yields  $T_b = 2T_1T_2/(T_1-T_2) = 2 \times 6.58 \times 4.69 / (6.58 - 4.69) = 32.66$  s or  $2 \times 6.9 \times 4.69 / (6.9 - 4.69) = 29.29$  s. These computed beating periods are shorter than the beating periods (between 50–150 s) observed from the response records depicted in Figure 4. The mismatch between observed and computed beating periods is significant but does not diminish that low damping is a cause of the observed long-duration beating vibrations.

Immediate remediation to improve the behavior and future resiliency of the building was accomplished by applying response modification technologies (e.g., adding dampers at select bays and floors) to dissipate vibrational energy and thus decrease the prolonged shaking and suppress the beating effect of the building during future strong shaking events.

### Case 2: Atwood Building, Anchorage, Alaska during Several Earthquakes

The Atwood Building, designed according to 1979 *Uniform Building Code (UBC)* and constructed in 1980 is a 20-story, 264 ft (80.5 m) tall steel moment-resisting framed (MRF) structure with only one level of basement. The building is 130ft x 130ft (39.6m x 39.6 m) in plan with a 48ft x 48ft (14.6m x 14.6m) center steel shear-walled core, and. The building foundation is without any piles and consists of a 5ft (1.52m) thick reinforced concrete mat below the core and a 4-ft 6-in. (1.37m) thick reinforced concrete perimeter mat interconnected with grade beams. A picture of the building, its three-dimensional schematic showing major dimensions, locations of accelerometers within the building and its associated downhole array is shown in Figure 6..

To date, more than two dozen earthquakes have been recorded by the building and downhole array ([www.strongmotioncenter.org](http://www.strongmotioncenter.org), last visited April 14, 2016). A comprehensive study of 19 earthquakes prior to August 2005 showed that there is close coupling between the translational and torsional modes. In general, the critical damping percentages were <5% (Çelebi, 2006). In this section, we use 3 of those 19 earthquake as well as the most significant recent M7.1 January 24, 2016 Iniskin (AK) earthquake. Table 2 summarizes particulars of the 4 earthquakes.

Figure 7 shows NS acceleration and displacement responses of the roof (Channel 30) for the first three events in Table 2. The three events are similar in magnitude and although they originate at different distances and azimuths, the amplitudes of accelerations and displacement responses and their corresponding amplitude spectra are comparable. Beating effects are observed in the responses of all three events.

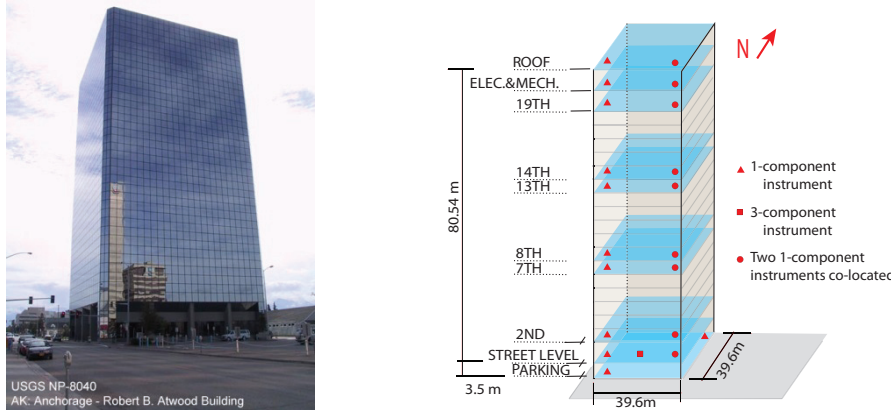


*Figure 6. (left) A photograph of the Atwood Building (Anchorage, AK). (right) Three-dimensional schematic of building showing the general dimensions and locations of accelerometers deployed within the structure. The superstructure array of this building's monitoring scheme is designed to capture (rocking) SSI effects in addition to the traditional translational and torsional responses.*

For event 3 in Table 2 (earthquake of April 6, 2005), Figure 8 shows spectral ratios of amplitude spectra of (a) NS and (b) EW accelerations (at the roof [CH30 and CH32] and 8<sup>th</sup> floor [CH15 and CH17] with respect to basement [CH2 and CH1] respectively) and (c) torsional accelerations at the roof [CH30-CH31] and 8<sup>th</sup> floor [CH15-CH16] with respect to those at the ground floor [CH5-CH7]. The range of the torsional frequencies [0.47-0.58 and 1.5-1.9 Hz] computed from differential accelerations are similar to the predominant frequencies [NS (0.58 and 1.8 Hz) and EW (.47 and 1.5 Hz) computed from NS and EW roof accelerations, strongly indicating coupling that resulted in significant beating effect displayed most prominently in the displacement time-history plots (Figure 7). Furthermore and similar to that of the building in Case 1, the narrow band of the structural frequencies in the spectral ratios reflect also the assessed low damping ratios. The translational frequencies and low damping percentages are further confirmed by system identification techniques. For the first two modes, Table 3 provides dynamic characteristics (including damping percentages) determined by system identification - details presented elsewhere (Çelebi, 2006). The reason why the second modal frequencies are included is mainly to show that associated damping percentages are low also for second modes.

**Table 2. Four of the Earthquakes Recorded by the Atwood Building Seismic Monitoring System. Building Coordinates: 61.21528 Latitude and 149.89296 Longitude. Only Processed Data Are Available at website [www.strongmotioncenter.org](http://www.strongmotioncenter.org) (Last Visited April 14, 2016). Azim.= Azimuthal Angle (Clockwise from North) to the Earthquake.**

Event No	Date	UTC	Event	Lat.	Long.	H km	Mw	Dist. km	Azim
1	2004/11/08	06:21	Denali Park	63.076	-151.425	9	4.9	222	340
2	2005/02/16	18:35	Pt. MacKenzie	61.337	-149.845	35	4.7	14	11
3	2005/04/06	17:51	Tazlina Glacier	61.454	-146.518	17	4.9	183	80
4	2016/01/24	10:30	Iniskin	59.659	-153.452	128	7.1	262	60

Thus, the beating period is difficult to accurately quantify since the translational and torsional frequencies are very close to one another. To provide a range of sample computations of beating frequency ( $f_b$ ) [period ( $T_b$ )], combinations of the translational frequency,  $f_1$  (period,  $T_1$ ) and torsional frequency,  $f_t$  (period,  $T_t$ ) are selected (Table 4). In the beating column of Table 1, the computed range of beating periods between 16-43 seconds is realistic when compared with those observed in the time-history plots shown in Figure 7.

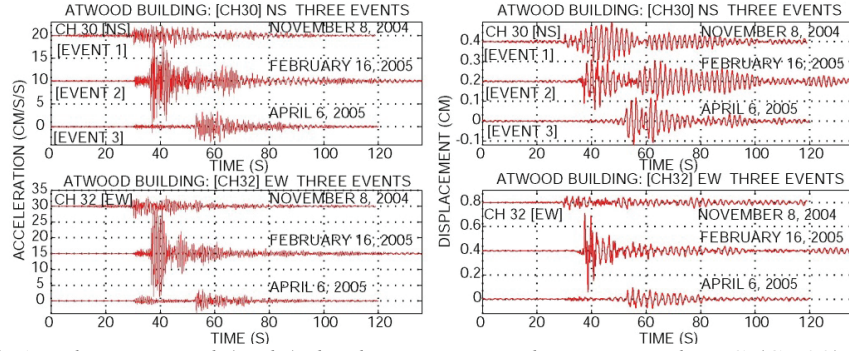


Figure 7. (left) Acceleration and (right) displacement time-histories in the NS (CH30) and EW (CH32) directions at the roof for the first three earthquakes (Table 2) that originate at varying distances and azimuths, all of which indicate a beating effect.

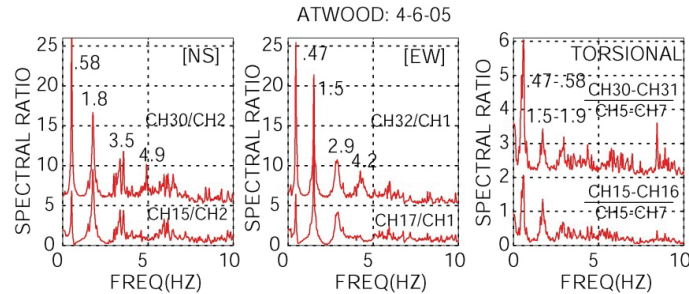


Figure 8. Spectral ratios computed from amplitude spectra of NS and EW accelerations at the roof (CH30 and CH32, respectively) and 8<sup>th</sup> floor (CH15 and 17) with respect to those at basement, and torsional accelerations at the roof and 8<sup>th</sup> floor with respect to those at ground floor (CH5 and 7).

**Table 3. Dynamic Characteristics Determined by System Identification – Event 3 ( $\xi$ =modal damping)**

Mode	NS			EW		
	$f$ (Hz)	$T$ (s)	$\xi$ (%)	$f$ (Hz)	$T$ (s)	$\xi$ (%)
1	0.53	1.89	2.7	0.47	2.13	4.2
2	1.83	0.55	2.7	1.53	0.65	2.8

**Table 4. Range of Beating Frequency ( $f_b$ ) and Period ( $T_b$ ) for Three Combinations of Translational and Torsional Frequencies Considered**

	Translational		Torsional		Beating	
	$f_1$ (Hz)	$T_1$ (s)	$f_t$ (Hz)	$T_t$ (s)	$f_b$ (Hz)	$T_b$ (s)
Combination 1	0.55	1.8	0.6	1.66	0.023	42.7
Combination 2	0.47	2.1	0.6	1.66	0.063	15.8
Combination 3	0.47	2.1	0.55	1.82	0.037	27.3

Listed as Event 4 in Table 2, the Iniskin (AK) earthquake also caused the responses of Atwood Building to display beating effects. Figure 9 shows acceleration and displacements time-histories at the roof in (left) NS and (center) EW directions. Particularly, the amplified displacements better display the beating periods. For example, for NS, between ~150-190 seconds, a beating cycle observation leads to ~ 40 s beating period. Figure 9 (right) shows amplitude spectra of roof accelerations in the NS (CH30 or CH31), EW (CH32) and torsional (CH30-CH31). The significant frequencies displayed expose how close the translational and torsional frequencies are (NS [0.48 Hz], EW [0.40 Hz] and torsional [~0.48Hz]). These frequencies are also confirmed by system identification analyses as summarized in Table 5.

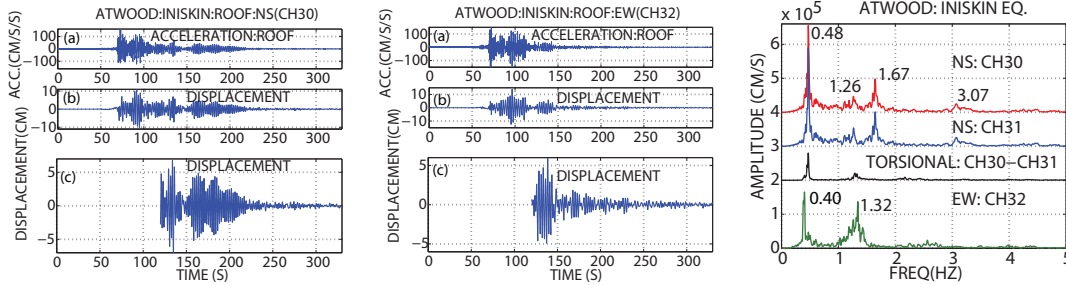


Figure 9. At the roof, (left) NS and (center) EW accelerations (top frames) and displacements (middle frames). For both NS and EW, the bottom frames are amplified plots of displacements to better display beating effect in the response of the building. (right) Amplitude spectra.

**Table 5. NS, EW and Torsional Modal Frequencies and Damping Percentages Computed by System Identification**

	Mode 1		Mode 2		Mode 3	
	$f$ (Hz)	$\xi$ (%)	$f$ (Hz)	$\xi$ (%)	$f$ (Hz)	$\xi$ (%)
NS1	0.47	1.47	1.65	2.52	3.12	1.98
EW	0.40	1.34	1.35	2.71	2.58	4.51
TOR	0.47	0.12	1.33	3.17	2.17	4.77

## Discussion and Conclusions

Although only two cases are presented in this paper, beating effects are often observed in records of prolonged responses of numerous tall or mid-rise buildings. In this paper, we draw attention to this real physical phenomenon that was observed in a building in Japan and another in the US. Quantification of the presence of beating can stimulate finding solutions to eliminate it, or to decrease the possible adverse effects that it may cause.

**Data Source and Disclaimer.** Japan data from <http://www.kyoshin.bosai.go.jp> (last visited April 21, 2016), US data from [www.strongmotioncenter.org](http://www.strongmotioncenter.org) (last visited May 4, 2016). Any use of trade, firm, or product names is for descriptive purposes only and does not imply endorsement by the U.S. Government.

## References

- Boroschek, R. L., and Mahin, S. A., 1991, Investigation of the seismic response of a lightly-damped torsionally-coupled building, University of California, Berkeley, *Earthquake Engineering Research Center Report*, UCB/EERC-91/18, 291pp.
- Çelebi, M., 2007, Beating Effect Identified from Seismic Responses of Instrumented Buildings, Proceedings of the American Society of Civil Engineers Structures Congress: New Horizons and Better Practices, Long Beach, California, 12 pages.

Çelebi, M., 1994, Response study of a flexible building using three earthquake records, *PROC. Structures Congress XII*, Atlanta, Georgia, pp. 1220-1225

Bendat, J.S., and Piersol, A.G., 1980, Engineering Applications of Correlation and Spectral Analyses, *John Wiley and Sons*, New York, New York, 302 pages.

Ljung, L., 1987, System Identification: Theory and User, *Prentice Hall*, Englewood Cliffs, New Jersey.

Çelebi, M., Okawa, I., Kashima, T., Koyama, S., and Iiba, M., 2014, Response of a tall building far from the epicenter of the March 11, 2011 M = 9.0 Great East Japan earthquake and its aftershocks, *The Wiley Journal of The Structural Design of Tall and Special Buildings*, pp. 23, 427-441.

Çelebi, M., 2006, Recorded Earthquake Responses from the Integrated Seismic Monitoring Network of the Atwood Building, Anchorage, Alaska, *Earthquake Spectra*.

Haskell, N. A., 1953, The dispersion of surface waves on multi-layered media, *Bull Seismological Society of America*, pp. 17-34.

Haskell, N. A., 1960, Crustal reflection of plane SH waves, *J. Geophysical Research*, pp. 4147-4150.